SYSTEM DEVELOPMENT OF MICROWAVE INDUCED THERMO-ACOUSTIC TOMOGRAPHY AND EXPERIMENTS ON BREAST TUMOR

Zhiqin Zhao[1, *], Jian Song[1], Xiaozhang Zhu[1], Jinguo Wang[1], Jiangniu Wu[1], Yulang Liu[1], Zaiping Nie[1], and Qinghuo Liu[2]

[1]School of Electronic Engineering, University of Electronic Science and Technology of China, Chengdu, Sichuan 611731, China

[2]Department of Electrical and Computer Engineering, Duke University, Durham, NC 27708, USA

Abstract—Microwave induced thermo-acoustic tomography (MITAT) has become a keen research topic in recent years due to its great potential in early breast cancer detection. A secure and accurate MITAT system has been established. Some experiments have been made to demonstrate the performance of the MITAT system. Based on an experiment using phantom, some quantitative features of the system have been obtained. Some imaging experiments with real human breast cancer tissues are performed to demonstrate its effectiveness and the potential in clinical diagnosis. Images with both high contrast and fine spatial resolution are achieved by using time reversal mirror (TRM) technique in the imaging processing. Moreover, comparisons between the MITAT system result and an ultrasound imaging system result are made. From the comparison, the MITAT system shows its advantages of better contrast over the ultrasound imaging system. The system and the experiments in this paper verify the mechanism of MITAT for breast cancer detection and provide a prototype basis for clinical practice.

1. INTRODUCTION

Microwave induced thermo-acoustic tomography (MITAT) has recently received more and more attentions due to its great potential in early breast cancer detection [1–5]. MITAT has the advantages of both high contrast of microwave imaging [6, 7] and fine resolution

of ultrasound imaging. In MITAT system, electromagnetic wave radiated by an antenna illuminates on a tissue. Then microwave energy absorbed by the tissue causes thermo-elastic expansion, which generates acoustic waves termed thermo-acoustic waves. An image which represents tissue's microwave absorption properties is reconstructed from the recorded thermo-acoustic signals. Because the microwave radiation absorption rates between tumors and normal tissues are quite different [8, 9], the thermo-acoustic image will have high contrast compared with that of acoustic imaging system which has been widely used. Near-field thermo-acoustic tomography system has great potentials for breast cancer imaging [10–13]. In the system, the imaged sample is placed in the vicinity of antenna to assure optimal near-field coupling. In this way, the losses by reflection and propagation are avoided.

A safe and efficient MITAT system is a foundation for obtaining a thermo-acoustic image with good quality. According to the mechanism of MITAT, the system is a combination of mechanics, microwave engineering, acoustic engineering and digital signal processing. In this paper, a near-field MITAT clinical prototype system has been firstly developed. The goal of the system is to build a platform which can experimentally demonstrate the advantages of MITAT and provide the basis for clinical practice.

In recent years, experiments on imaging real human tissue of MITAT have attracted lots of attentions [5, 14]. Some thermo-acoustic imaging results for various kinds of phantoms were reported to demonstrate MITAT's potential in breast tumor detection [2–5]. It requires that the electromagnetic parameters and acoustic properties of a phantom must be similar to a real tissue. However, this is always very difficult. The best way is to use real tissues. In [5, 14], although a malignant breast tissue was imaged by the thermo-acoustic signals and compared with a radiograph, the freshness of the specimens is not mentioned. If the electromagnetic parameters of the specimen are very different from the tissue *in vivo*, the meaning to the clinical practice is limited. Furthermore, the experimental device in [5] is only a laboratorial appliance, some components such as microwave antenna etc. need to be improved for clinical practice.

In this paper, in order to validate the effectiveness and the potential in clinic diagnosis, a MITAT system has been established. Experiments with both phantom and real human breast cancer tissues are performed. In theory, in order to obtain the best angle resolution, the ultrasound transducers have to be aligned horizontally as a circular array with $\lambda/2$ spacing. (λ is the wavelength of the received acoustic signal. It is at the level of mm). However, it is hard to meet this

requirement due to the large diameter of the ultrasound transducer. So a concept of synthetic aperture is applied. A scanning system has been developed to collect the signals at different angles which are used to form a virtual circular array. The developed scanning platform has a step accuracy of 0.00625°. Because the amplitude of the collected signal of MITAT is at the level of µV, a low-noise pre-amplifier is necessary and important for the system. A low-noise pre-amplifier with 86 dB gain is developed for the system in this paper. Imaging method is another important issue for a good MITAT system. Time Reversal Mirror (TRM) technique is applied as an inversion method to reconstruct the image. TRM is a combination technique based on wave propagation and array signal processing [15–18]. It has the ability to effectively suppress system noise because of its characteristics of spatial-temporal matched filtering compared with other methods. Furthermore, due to its self-average property, TRM has the statistic stability even in slightly heterogeneous media.

In order to test the performance of the developed MITAT system, a phantom is applied to verify the main performances of the system such as contrast, spatial resolution and positioning accuracy etc.. Aiming to assure the electromagnetic parameters of the tissues much closer to that of the tissues *in vivo*, we adopt fresh cancer tissue specimens to perform the experiments. The tissue specimens in the experiments include normal breast tissue specimens and breast cancer tissue specimens. In order to demonstrate the advantages of the MITAT in breast tumor detection, an experiment on ultrasound imaging system are made as comparisons.

The remainder of the paper is organized as follows. In Section 2, a developed MITAT system is briefly described. Some important parameters and sub-systems are discussed. Based on an experiment using phantom, some quantitative features of the system have been obtained. Real breast tissue specimens and the corresponding electromagnetic parameters are given in Section 3. Some imaging experiments with real human breast cancer tissues are performed and analyzed in Section 4. Conclusions are drawn in the last section.

2. MITAT SYSTEM

2.1. Constitution of MITAT System

The structure chart of the MITAT system is illustrated in Fig. 1. The MITAT system mainly consists of microwave radiation part, thermo-acoustic acquisition subsystem and signal processing component. All these subsystems are carefully designed to develop a secure and accurate system. The microwave radiator is designed to radiate the
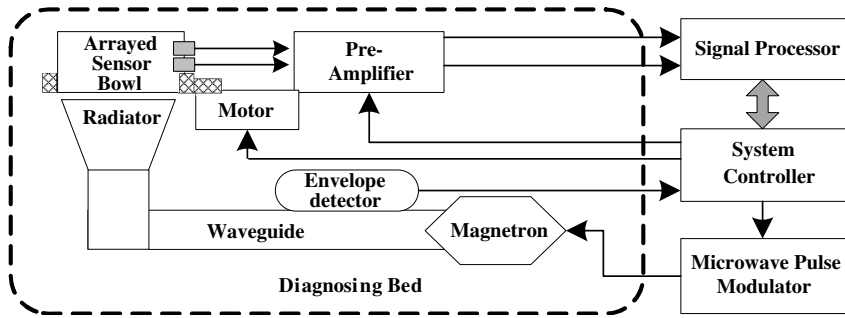
Figure 1. Structure chart of MITAT system.

microwave pulse as uniformly as possible. The signal acquisition and processing components are developed to accurately acquire the thermo-acoustic signals and reconstruct the image.

The working procedures of the MITAT system are summarized as follows. In a scanning procedure, the system controller controls the motor to drive the scanning bowl to rotate a scanning step. Afterwards, the trigger pulses are sent from the system controller to trigger the microwave modulator and the data acquisition card. The irradiated microwave from the radiator illuminates on a tissue in the bowl. Thermo-acoustic signals will be generated due to thermo-elastic expansion of the tissue. The thermo-acoustic signals are sampled and recorded in the computer. After finish all the scanning procedures, the digital thermo-acoustic signals are processed to reconstruct an image in the signal processor.

2.2. Designs of Key Parts in MITAT System

Figure 2 is a picture of the MITAT system prototype developed by our research team. A 2.45 GHz microwave generator transmits microwave pulses toward a specimen. The pulse duration time is set to be 0.5 µs with an adjustable switch in the experiments. A rectangle pulse modulator is employed to trigger the microwave generator and to control the pulse repetition rate. In this way, the microwave radiation energy can be well controlled. Microwave energy is delivered to the radiator through a standard rectangular waveguide. A circular horn antenna is designed as used as the radiator, which is designed to radiate the microwave energy as equally as possible in the container to heat the sample at different position with the same power.

A circular container is designed inside which a tissue is located. Acoustic sensors are aligned on the wall of the container to acquire acoustic signals radiated by the tissue. As the size of the acoustic
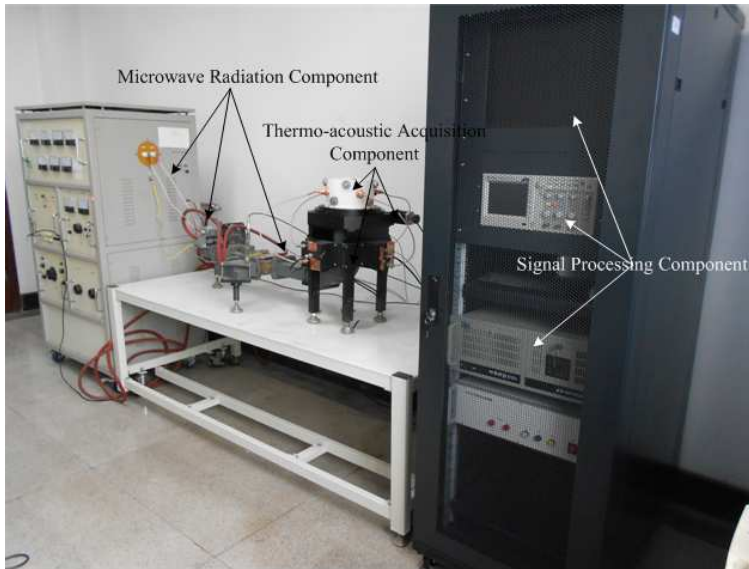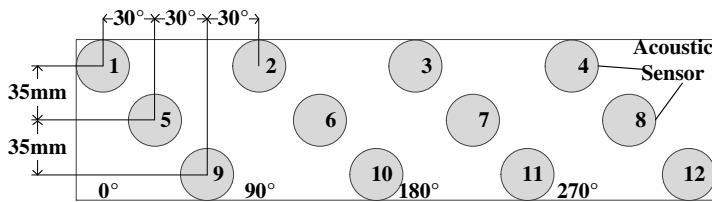
Figure 2. Picture of the MITAT system.

Figure 3. Cylindrical expansion view of the sensors aligned on the wall of the container.

transducer is much larger than the wavelength of the acoustic wave, a circular scanning system is adopted in order to implement the requirement of half wavelength spacing between the sensors. (According to the frequency range of thermo-acoustic signal of the breast tissue, the array spacing needs to be less than 2.5 mm). Usually, the amplitude of the thermo-acoustic signal emitted from the tissue is very weak (at the level of tens of μV). The circular design of the array will equivalently increase the aperture of the receiver array, which will significantly increase signal noise ratio (SNR). Cylindrical expansion view of the sensors aligned on the wall of the container is illustrated in Fig. 3.

The specimen (tissue) to be imaged is placed in the container,

which is fixed on the horizontal scanning plane. The container is driven by a stepping motor to rotate with variable steps. Acoustic signals are received by the ultrasound transducers at each scanning during the rotation. After 90° rotation, the sampled data of all sensors can be synthesized into a circular aperture with small arc spacing.

A controlling module is designed to control the motor to drive the scanning device. According to the Nyquist's Sampling Theorem, the arc spacing should be less than half wavelength of the thermo-acoustic signal. Therefore in the prototype system, the accuracy and precision of the circular scanning platform should be finer than 1 mm. A circular scanning platform with worm-drive transmission was developed to solve the problem. The structure provides a 288 : 1 transmission ratio. When the worm-shaft is driven by a step motor with 1.8° per-step, the worm-wheel will have 0.00625° step accuracy, about 0.015 mm arc spacing accuracy on the scanning container. This feature satisfies the requirement of the sensor array.

The acoustic signals received by the ultrasound transducers are acquired by a general purpose 4-channel data acquisition card (PCI-1714, ADVANTECH). The central frequency of the ultrasound transducer (V314-SU, OLYMPUS) is 1 MHz. The piezoelectric output of the ultrasound transducer is connected to a pulse amplifier. A low noise pulse amplifier has been researched and fabricated. The main electric parameters of the amplifier are listed in Table 1.

2.3. Digital Thermo-acoustic Signal Processing

The initial microwave absorption properties of the tissue are reconstructed by using TRM technique. The application of TRM in

Table 1. Parameters of pre-amplifier.

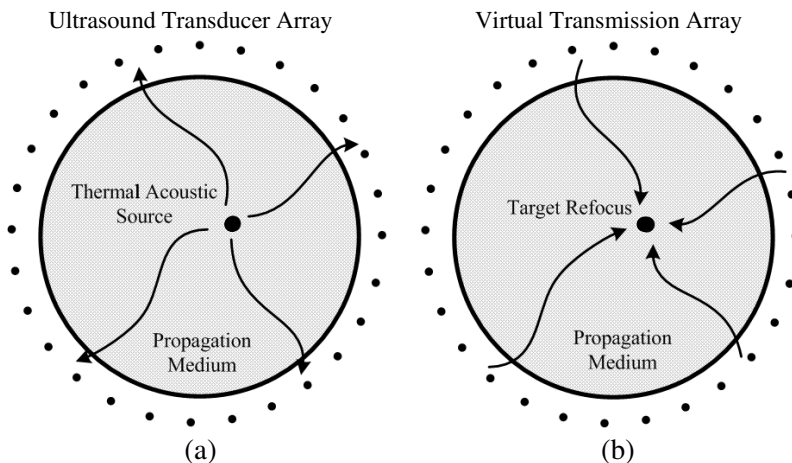| Gain	86dB (20000)
High-pass frequency	$30 \pm 0.5\,\text{kHz}$
Low-pass frequency	$5.7 \pm 0.2\,\text{MHz}$
Input impedance	$100\,\text{K}\Omega$
Output impedance	$50\,\Omega$
Noise floor RMS	$70\,\text{mV}$
Output V_{pp}	$7.32\,\text{V}$
Gain miss match between channels	$< 1\,\text{dB}$
Pass band ripple	$< 1\,\text{dB}$
Stop band attenuation	$> 40\,\text{dB/0\,ct}$

Figure 4. Fundamental of TRM in MITAT. (a) Forward procedure; (b) Inverse procedure.

tomography was initially suggested by Xu and Wang [19]. A great deal of work has been done to demonstrate the feasibility of TRM technique being used as an imaging algorithm for MITAT [15–20]. The fundamental of the TRM in MITAT system can be explained by Fig. 4. Fig. 4(a) indicates that the thermo-acoustic signals propagate through a medium and are received by the ultrasonic transducers around the tissue. The received thermo-acoustic signals are transmitted back into the imaging area with a virtual transducer array. According to the reciprocity theorem, the received thermo-acoustic signals will be refocused at the location of the initial acoustic source. The process of refocusing is shown in Fig. 4(b). More details can be referred in [15].

The phantom, which has the similar electromagnetic parameters with tumor, is a good choice for thermo-acoustic imaging experiment [21] to test the imaging ability of the MITAT system. Pictures of the phantom and the achieved thermo-acoustic image are shown in Fig. 5.

The main features of the MITAT system are summarized in Table 2. The contrast is defined as the ratio between the pixel mean value in the target zone and the pixel mean value of the background.

3. EXPERIMENTAL BREAST TISSUES

In the previous section, experiments with phantom have been made to test the capability of the system. In order to further demonstrate the ability of the system, experiments with real tumor tissues are explored.

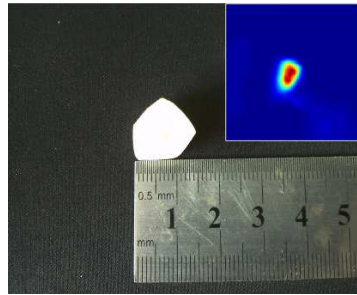Different electromagnetic parameters of cancer and normal tissues

Figure 5. Picture of the phantom, the inset one is the thermo-acoustic image by using MITAT system.

Table 2. Performance of the MITAT system.

Microwave average power:	15 mw
Contrast (phantom : background):	383 : 1
Spatial resolution:	1 mm
Positioning accuracy:	< 1 mm
Amplifier gain:	86 dB

are the foundation for the detection with MITAT. Thermo-acoustic pressure waves, induced via local heat deposition by microwave energy absorption, can be described via the thermo-acoustic wave equation [12], i.e.,

$$\nabla^2 p\left(\vec{r}, t\right) - \frac{1}{v_s^2}\frac{\partial^2 p\left(\vec{r}, t\right)}{\partial t^2} = -\frac{\beta}{C}\frac{\partial H\left(\vec{r}, t\right)}{\partial t}, \tag{1}$$

with $p(\vec{r}, t)$ the induced pressure, $H(\vec{r}, t)$ the heating function, v_s the sound speed, C the specific heat capacity and β the thermal expansion coefficient, defined as the relative volume change with temperature under constant pressure. Assuming detector position at $\vec{r}'$ around the object with source points being positioned at $\vec{r}$, the three-dimensional wave Equation (1) can be solved with volume integration

$$p\left(\vec{r}', t\right) = \frac{\beta}{4\pi C}\iiint\limits_{V} \frac{1}{|\vec{r} - \vec{r}'|}\frac{\partial H\left(\vec{r}, t'\right)}{\partial t'}dV \tag{2}$$

at time $t' = t - |\vec{r} - \vec{r}'|/v_s$. Under thermal stress confinement, the heating function can be rewritten in the form with product separated contribution of the spatial $H(\vec{r})$ and temporal $\delta(t')$ parts.

$$\frac{\partial H(\vec{r}, t')}{\partial t'} \approx H(\vec{r})\frac{\partial \delta(t')}{\partial t'}. \tag{3}$$

The heating function can be described as the deposition of microwave power in the sample [12]

$$H\left(\vec{r}\right) = \frac{\sigma\left(\vec{r}\right)}{2}\left|\vec{E}_{\vec{r}}\right|^2 \Delta V + \frac{\omega\varepsilon_r''\left(\vec{r}\right)}{2}\left|\vec{E}_{\vec{r}}\right|^2 \Delta V + \frac{\omega\mu_r''\left(\vec{r}\right)}{2}\left|\vec{H}_{\vec{r}}^{mag}\right|^2 \Delta V, \quad (4)$$

where the first term of the right hand is the conductivity losses with the conductivity of sample $\sigma(\vec{r})$, the second term is the dielectric losses with the imaginary part of the sample permittivity $\varepsilon_r''(\vec{r})$, the third term is the magnetic losses with the imaginary part of the sample permeability $\mu_r''(\vec{r})$, ω is the angular frequency, ΔV is unit volume cell, $\vec{E}_{\vec{r}}$ is the electrical field and $\vec{H}_{\vec{r}}^{mag}$ is the magnetic field.

Equation (4) takes into account the conductivity losses, the dielectric losses and the magnetic losses. Neglecting magnetic losses, Equation (4) indicates that the intrinsic contrast in thermo-acoustic tomography is dominated by electric losses in the imaged sample. In early breast cancer detection, the physical parameters (β, C_V, v_s) have low variation in soft tissue and can usually be neglected for contrast [22]. Thus, the objects with high conductivity have higher energy absorption than tissue with lower conductivity. Therefore, the resulting thermo-acoustic image maps conductivity distribution in the image [12]. Table 3 gives the electromagnetic parameters of some breast tissues [8, 14]. The conductivity ratio between tumor and fatty breast tissue is 10.

Aiming to study the biological tissue imaging performance of MITAT system, breast cancer tissue and normal tissue are used in the experiments. In the experiments, the sizes of tissues are millimeter level in order to correspond with the size of early breast tumor. Two sets of samples are used. The first set is a cancer tissue which is shown in Fig. 6(a). The specimen is adopted to perform the imaging experiment within two hours after the surgery and its cross section size is about $10\,\text{mm} \times 10\,\text{mm}$. The size is corresponding to that of the early breast tumor. It is used to verify the feasibility of MITAT for early breast tumor. Another set of samples is a cancer breast tissue and a

Table 3. Dielectric properties of breast tissues.

Tissues	Dielectric Properties	
	Relative Permittivity	Conductivity (S/m)
Skin	36	4
Fatty Breast Tissue	9	0.4
Glandular Tissue	11–15	0.4–0.5
Tumor	50	4

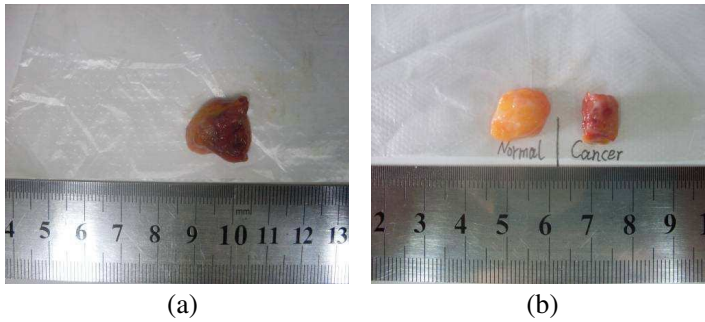(a)   (b)

Figure 6. The tissue samples for experiments. (a) Cancer tissue; (b) Normal and cancer tissues.

normal breast tissue. They are used to perform imaging experiment at the same time in order to observe the contrast of MITAT for different tissues. This contrast experiment provides basis for the clinical tumor detection from breast fatty tissue. The cross section sizes of the tissues are both about $10\,\text{mm} \times 5\,\text{mm}$. The optical picture of this set of tissues is shown in Fig. 6(b).

4. EXPERIMENTAL RESULTS AND ANALYSES

The cancer tissue (Fig. 6(a)) irradiated by microwave pulses generates the thermo-acoustic signal which is shown in Fig. 7(a). This thermo-acoustic signal is a classical bipolar signal which agrees with the reported thermo-acoustic signals in [14]. Other waveforms after the thermo-acoustic signal are generated by the interference occurred in the ultrasound transducer. These waveforms are filtered in the image reconstruction procedure because of the spatial-temporal matched filtering characteristics in TRM technique. The components with very large amplitude during $0 \sim 10\,\mu\text{s}$ before the thermo-acoustic are due to the microwave interferences. They can be filtered out before the image reconstruction.

TRM technique is approached as the image reconstruction algorithm. The reconstructed image for the cancer tissue (as shown Fig. 6(a)) is shown in Fig. 7(b). It can be found that the boundary of cancer tissue is distinguished clearly. In Fig. 7(b), the spatial resolution is about $1.74\,\text{mm}$. This high resolution benefits from the super resolution property of TRM technique [23]. The good spatial resolution of thermo-acoustic image also benefits from the large aperture size of the circular array.
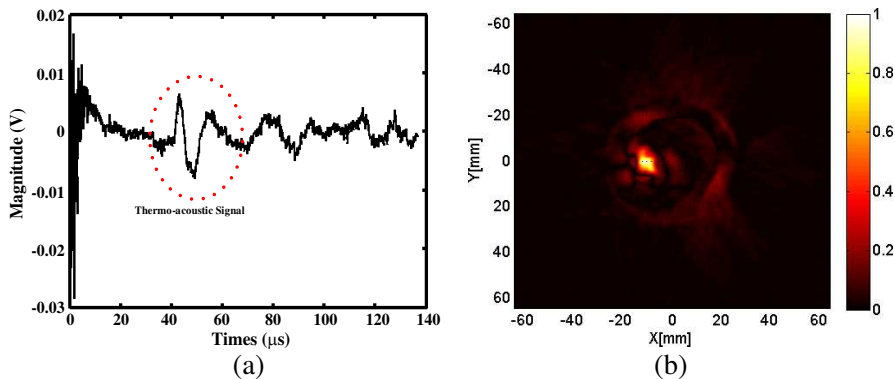
Figure 7. (a) Thermo-acoustic signal generated by cancer tissue; (b) Reconstructed image of the cancer.
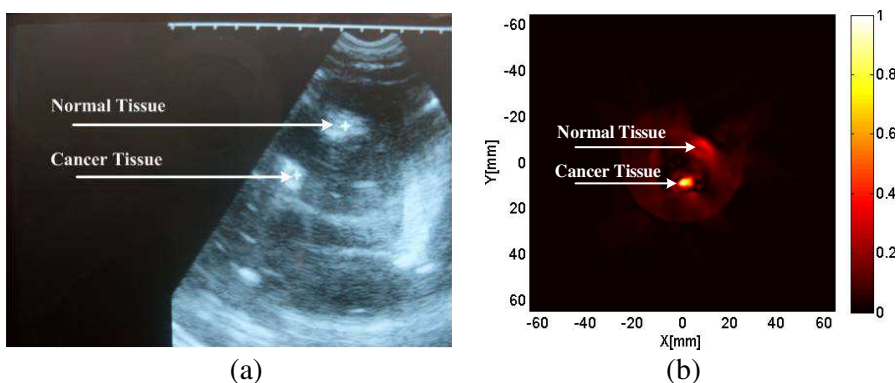

Figure 8. (a) Ultrasonic image; (b) Thermo-acoustic image.

In order to compare the thermo-acoustic image to the ultrasound image, an ultrasound imaging system is used to image the tissues. The ultrasound imaging system is a commercial linear array ultrasound system (CX_130D, HuaXi) whose ultrasound central frequency is 3.5 MHz. The ultrasound imaging system has satisfactory resolution for its short ultrasound wavelength. The ultrasound image obtained from this system is used to compare with the thermo-acoustic image.

Figure 8(a) is the ultrasound image for the tissues shown Fig. 6(b). This image is generated by ultrasound imaging system. In the ultrasound image, the contrast between the cancer tissue and the normal tissue is not obvious. One can not make a distinction between the cancer tissue and the normal tissue from the ultrasound image.

The ultrasound detection based on the acoustic parameters could not well distinguish the cancer tissue from the normal tissue due to their minor difference in sound velocity. However, the thermo-acoustic imaging based on the electromagnetic parameters has significantly better contrast between the cancer tissue and normal tissue. The thermo-acoustic image for this set of tissues (the picture of the tissues is shown in Fig. 6(b)) is shown in Fig. 8(b). It can be found that the image contrast between the cancer tissue and the normal tissue is more than 12 dB, which closely reflects the electromagnetic parameters of the normal and cancer tissues [24]. This comparison between thermo-acoustic imaging and ultrasound imaging indicates that the thermo-acoustic image has very strong advantage on high contrast.

5. CONCLUSION

In this paper, a design of a MITAT system and its features are briefly introduced. A concept of synthetic aperture is applied to the system by using a scanning mode. This design effectively overcomes the limitation of large transducer diameter and obtains the best angle resolution. The feasibility for early breast cancer detection in MITAT is verified by the imaging experiments of a tumor specimen. Experimental results show that tissues with sufficiently dielectric contrast can be well imaged using this MITAT system. The advantage on contrast of MITAT system is demonstrated by the experiment with a set of cancer breast tissue and normal breast tissue. This experiment also indicates that the MITAT system has the potential to distinguish the tumor from the breast fatty tissue. The comparison between thermo-acoustic image and ultrasound image demonstrates the advantage of MITAT on contrast. The MITAT system with the advantages of high contrast and resolution can be potentially developed as a reliable, fast and low-cost imaging clinical apparatus for early stage breast cancer detection and imaging.

REFERENCES

1. Guo, B., J. Li, H. Zmuda, and M. Sheplak, "Multifrequency microwave-induced thermal acoustic imaging for breast cancer detection," *IEEE Trans. Biomed. Eng.*, Vol. 54, No. 11, 2000–2010, 2007.

2. Geng, K. and L. V. Wang, "Scanning microwave-induced thermoacoustic tomography: Signal, resolution, and contrast," *Med. Phys.*, Vol. 28, No. 1, 4–10, 2001.

3. Geng, K. and L. V. Wang, "Scanning thermoacoustic tomography in biological tissue," *Med. Phys.*, Vol. 27, No. 5, 1195–1202, 2000.

4. Nie, L. M., D. Xing, D. W. Yang, L. M. Zeng, and Q. Zhou, "Detection of foreign body using fast thermo-acoustic tomography with a multi-element linear transducer array," *Appl. Phys. Lett.*, Vol. 90, 174109–174111, 2007.

5. Nie, L. M., D. Xing, Q. Zhou, D. W. Yang, and H. Guo, "Microwave-induced thermoacoutic scanning CT for high-contrast and noninvasive breast cancer imaging," *Med. Phys.*, Vol. 35, No. 9, 4026–4032, 2008.

6. Zhu, G. K. and M. Popovic, "Comparison of radar and thermoacoustic technique in microwave breast imaging," *Progress In Electromagnetics Research B*, Vol. 35, 1–14, 2011.

7. Catapano. I., L. Di Donato, L. Crocco, O. M. Bucdi, A. F. Morabito, T. Isernia, and R. Massa, "On quantitative microwave tomography of female breast," *Progress In Electromagnetics Research*, Vol. 97, 75–93, 2009.

8. Lazebnik, M., "A large-scale study of the ultrawideband microwave dielectric properties of normal, benign and malignant breast tissues obtained from cancer surgeries," *Phys. Med. Biol.*, Vol. 52, 6093–6115, 2007.

9. Geng, K., B. D. Fornage, X. Jin, M. Xu, K. K. Hunt, and L. V. Wang, "Thermoacoustic and photoacoustic tomography of thick biological tissues toward breast imaging," *Technol. Cancer Res. Treat.*, Vol. 4, 1–7, 2005.

10. Yan, W., J.-D. Xu, N.-J. Li, and W.-X Tan, "A novel fast nearfield electromagnetic imaging method for full rotation problem," *Progress In Electromagnetics Research*, Vol. 120, 387401, 2011.

11. Qi, Y. L., W. Tan, Y. Wang, W. Hong, and Y. Wu, "3D bistatic Omega-K imaing algorithm for near range microwave imaging system with bistatic planar scanning geometry," *Progress In Electromagnetics Research*, Vol. 121, 409–431, 2011.

12. Kellnberger, S., A. Hajiaboli, D. Razansky, and V. Ntziachristos,

"Near-field theroacoustic tomography of small animals," *Phys. Med. Biol.*, Vol. 56, 3433–3444, 2011.

13. Razansky, D., S. Kellnberger, and V. Ntziachristos, "Near-field radiofrequency thermo-acoustic tomography with impulse excitation," *Med. Phys.*, Vol. 37, No. 9, 4602–4607, 2010.

14. Xie, Y., B. Guo, and J. Li, "Adaptive and robust methods of reconstruction (ARMOR) for thermo-acoustic tomography," *IEEE Trans. Biomed. Eng.*, Vol. 55, 2741–2752, 2008.

15. Chen, G. P., Z. Q. Zhao, Z. P. Nie, and Q. H. Liu, "Computational study of time reversal mirror technique for microwave-induced thermo-acoustic tomography," *Journal of Electromagnetic Waves and Applications*, Vol. 22, No. 16, 2191–2204, 2008.

16. Chen, G. P., W. B. Yu, Z. Q. Zhao, Z. P. Nie, and Q. H. Liu, "The prototype of microwave-induced thermo-acoustic tomography imaging by time reversal mirror," *Journal of Electromagnetic Waves and Applications*, Vol. 22, Nos. 11–12, 1565–1574, 2008.

17. Chen, G. P., Z. Q. Zhao, W. J. Zheng, Z. Nie, and Q. H. Liu, "Application of time reversal mirror technique in microwave-induced thermo-acoustic tomography system," *Science in China Series E: Technological Science*, Vol. 52, No. 7, 2087–2095, 2009.

18. Treeby, B. E. and B. T. Cox, "K-wave: MATLAB toolbox for the simulation and reconstruction of photo-acoustic wave fields," *Journal of Biomedical Optics*, Vol. 15, No. 2, 021314, 2010.

19. Xu, Y. and L. V. Wang, "Time reversal and its application to tomography with diffracting sources," *Phys. Rev. Lett.*, Vol. 92, No. 3, 1–4, 2004.

20. Fink, M. and C. Prada, "Acoustic time reversal mirror," *Inv. Probl.*, Vol. 17, No. 1, 1–38, 2001.

21. D'Souza, W. D., E. L. Madsen, O. Unal, et al., "Tissue mimicking materials for a multi-imaging modality prostate phantom," *Med. Phys.*, Vol. 28, No. 4, 688–700, 2001.

22. Bauer, D., X. Wang, J. Vollin, H. Xin, and R. Witte, "Spectroscopic thermoacoustic imaging of water and fat composition," *Appl. Phys. Lett.*, Vol. 101, 033705, 2012.

23. Blomgren, P., G. Papanicolaou, and H. Zhao, "Super-resolution in time-reversal acoustics," *Journal of the Acoustical Society of America*, Vol. 111, 230–248, 2002.

24. Halter, R. J., T. Zhou, P. M. Meaney, et al., "The Correlation of in vivo and ex vivo tissue dielectric properties to validate electromagnetic breast imaging: Initial clinical experience," *Physiol. Meas.*, Vol. 30, No. 6, 121–136, 2009.